

PAPER • OPEN ACCESS

Global crop yield response to extreme heat stress under multiple climate change futures

To cite this article: Delphine Deryng *et al* 2014 *Environ. Res. Lett.* **9** 034011

View the [article online](#) for updates and enhancements.

You may also like

- [Potential change in forest types and stand heights in central Siberia in a warming climate](#)
N M Tchebakova, E I Parfenova, M A Korets *et al.*
- [Heat stress, labour productivity and adaptation in Europe—a regional and occupational analysis](#)
Wojciech Szewczyk, Ignazio Mongelli and Juan-Carlos Ciscar
- [Streamflow response under different climate change scenarios in data-scarce White Volta basin of West-Africa using a semi-distributed hydrologic model](#)
S Abubakari, X Dong, J Liu *et al.*

Recent citations

- [Optimizing Sowing Date and Planting Density Can Mitigate the Impacts of Future Climate on Maize Yield: A Case Study in the Guanzhong Plain of China](#)
Fang Xu *et al*
- [Increasing Human Perceived Heat Stress Risks Exacerbated by Urbanization in China: A Comparative Study Based on Multiple Metrics](#)
Ming Luo and NgarCheung Lau
- [Analysing the resilience of agricultural production systems with ResiPy, the Python production resilience estimation package](#)
Matteo Zampieri *et al*

Global crop yield response to extreme heat stress under multiple climate change futures

Delphine Deryng^{1,2}, Declan Conway³, Navin Ramankutty⁴, Jeff Price² and Rachel Warren^{1,2}

¹ Tyndall Centre for Climate Change Research, University of East Anglia, Norwich, NR4 7TJ, UK

² School of Environmental Sciences, University of East Anglia, Norwich, NR4 7TJ, UK

³ Grantham Research Institute on Climate Change and the Environment, London School of Economics and Political Science, WC2A 2AE, London, UK

⁴ Department of Geography and Global Environmental and Climate Change Centre, McGill University, Montreal, Canada

E-mail: d.deryng@uea.ac.uk

Received 10 November 2013, revised 20 February 2014


Accepted for publication 21 February 2014

Published 19 March 2014

Abstract

Extreme heat stress during the crop reproductive period can be critical for crop productivity. Projected changes in the frequency and severity of extreme climatic events are expected to negatively impact crop yields and global food production. This study applies the global crop model PEGASUS to quantify, for the first time at the global scale, impacts of extreme heat stress on maize, spring wheat and soybean yields resulting from 72 climate change scenarios for the 21st century. Our results project maize to face progressively worse impacts under a range of RCPs but spring wheat and soybean to improve globally through to the 2080s due to CO₂ fertilization effects, even though parts of the tropic and sub-tropic regions could face substantial yield declines. We find extreme heat stress at anthesis (HSA) by the 2080s (relative to the 1980s) under RCP 8.5, taking into account CO₂ fertilization effects, could double global losses of maize yield ($\Delta Y = -12.8 \pm 6.7\%$ versus $-7.0 \pm 5.3\%$ without HSA), reduce projected gains in spring wheat yield by half ($\Delta Y = 34.3 \pm 13.5\%$ versus $72.0 \pm 10.9\%$ without HSA) and in soybean yield by a quarter ($\Delta Y = 15.3 \pm 26.5\%$ versus $20.4 \pm 22.1\%$ without HSA). The range reflects uncertainty due to differences between climate model scenarios; soybean exhibits both positive and negative impacts, maize is generally negative and spring wheat generally positive. Furthermore, when assuming CO₂ fertilization effects to be negligible, we observe drastic climate mitigation policy as in RCP 2.6 could avoid more than 80% of the global average yield losses otherwise expected by the 2080s under RCP 8.5. We show large disparities in climate impacts across regions and find extreme heat stress adversely affects major producing regions and lower income countries.

Keywords: climate impacts, global crop yield, extreme temperature stress

 Online supplementary data available from stacks.iop.org/ERL/9/034011/mmedia



Content from this work may be used under the terms of the [Creative Commons Attribution 3.0 licence](https://creativecommons.org/licenses/by/3.0/). Any further distribution of this work must maintain attribution to the author(s) and the title of the work, journal citation and DOI.

1. Introduction

Anthropogenic climate change challenges current and future global food production due to the direct effects of changes

in mean climatic conditions, increasing risks from extreme weather events, increased atmospheric CO₂ concentration and increasing pest damage [1, 2]. The Fourth Assessment Report (AR4) of the Intergovernmental Panel on Climate Change (IPCC) reports moderate increase in global crop yield for global mean temperature increase up to 3 °C—mostly due to beneficial CO₂ fertilization effects on photosynthesis rate and transpiration demand—but general decrease above this threshold [3]. The report further concludes projected changes in the frequency and severity of extreme climatic events will have more serious consequences for food production and food insecurity, than changes in mean climate alone [3].

Yet global climate impact assessments to date fail to address adequately effects of changes in climate extremes on crops [1, 2, 4–7], especially the negative impact of heat waves during the reproductive stage, identified as a major threat to yield in many parts of the world. Previous analyses modelling the effect of extreme heat stress on crops have been limited to single regions [8–12] or do not quantify impacts on yield [13, 14]. Moreover, most previous studies present only a partial estimate of uncertainty related to the range of climate change projections by considering at most four global climate models (GCMs) using the older SRES emissions scenarios [3, 4, 6, 7]. Finally, anticipated benefits from CO₂ fertilization effects remain a large source of uncertainty [15].

Here we use a new version of the global crop yield model PEGASUS [5] that takes into consideration heat stress sensitivity around crop anthesis (HSA) [10, 16] and CO₂ fertilization effects for maize, spring wheat and soybean. We use an ensemble of 72 climate change projections spanning the 21st century together with the CRU TS 2.10 observed climate dataset [17] for the years 1971–2000 to drive PEGASUS and produce a robust estimate of uncertainties related to future climate change. Our approach takes into account impacts of change in mean climate conditions, extreme temperatures and elevated atmospheric CO₂ concentration. We explore PEGASUS' sensitivity to HSA and CO₂ fertilization effects and show impacts on global crop yield and production on present-day harvested areas. We present results from different Representative Concentration Pathways (RCPs) [18] to evaluate potential benefits of mitigation policy. Although we make use of one single global gridded crop model and do not evaluate across-model uncertainty, PEGASUS enables a first assessment of the effect of HSA on global crop productivity, currently missing in other comparable state-of-the-art global gridded crop models [19]. Key sources of uncertainty resulting from the use of a single crop model (i.e., consisting primarily of uncertainty in the magnitude of CO₂ fertilization effects, temperature thresholds for HSA, and model representation of water, temperature and nitrogen stresses), the use of static harvested areas, and assumptions about farmers' adaptation responses (i.e., decision of planting dates and choice of crop cultivars) are addressed in the discussion section.

2. Methods

2.1. Crop modelling

PEGASUS 1.1 is an improved version of the global crop yield model PEGASUS [5] that simulates crop response

to elevated CO₂ and better represents effects of climate variability and extremes. A specific heat stress factor is calculated as a function of intensity and duration of extreme temperature events during crop anthesis according to crop specific temperature thresholds [10, 14, 16] (see appendix A). A literature review indicates spring wheat starts to face HSA at a lower critical temperature (T_{cr}) threshold than for the other crops and maize can tolerate a higher limit temperature (T_{lim}) (table A.1). Soybean experiences a shorter range of elevated temperatures and a steeper decline in yield between the critical threshold and limit temperatures (table A.1).

Farm management practices represented in PEGASUS include irrigation and fertilizer application, decision of planting dates and choice of crop cultivars. Our simulations allow for adaptation in decision of planting dates and choice of crop cultivars, according to temperature and precipitation conditions as in Deryng *et al* [5]. In temperature-limited regions, PEGASUS typically allows for earlier sowing dates and longer growing season varieties due to warming temperatures. In moisture-limited regions, PEGASUS tends to coincide sowing dates with the start of the rainy season (the crop calendar methodology is described in detail in [5]). As a result of adaptation of planting dates and cultivars, timing of crop anthesis can vary with climate change and thus influences net HSA effects on crops: temperature-limited regions show unchanged or slightly later flowering dates resulting mainly from longer growing periods, which is more influential than the effect of earlier planting; moisture-limited regions tend to show earlier flowering dates resulting from earlier planting dates (Figure S1 in the SI available at stacks.iop.org/ERL/9/034011/mmedia).

Total harvested area, along with fraction of total irrigated and rainfed areas, are kept constant to present-day (circa the year 2000) and irrigation water is applied to prevent irrigated crops from experiencing water stress, assuming unlimited availability of irrigation water as in Deryng *et al* [5]. We use the Earthstat dataset (www.earthstat.org) for global crop harvested area [20] in combination with the MIRCA2000 dataset [21] for crop specific irrigated areas to define present-day harvested areas and fraction of irrigated and rainfed areas. Similarly, we use national annual rates of NPK (i.e., combining nitrogen, phosphate and potash) fertilizer application from the International Fertilizer Industry Association (IFA) [22] corresponding to the mid-1990s and maintain application rates constant throughout the simulations.

PEGASUS is calibrated and validated for the year 2000 using the CRU TS 2.10 climate data [17] for the period 1997–2002 and the Earthstat dataset for global crop yield and harvested area [20]. Average simulated crop yield for the period 1997–2002 is used to approximate yield for the year 2000.

2.2. Climate modelling

PEGASUS is driven by climate data from the CRU TS 2.10 dataset for the period 1971–2000 and from the Community Integrated Assessment System (CIAS) [23] for the period 2001–2100. CIAS uses greenhouse gas (GHG) emissions time

series corresponding to the four RCPs emission scenarios [18] to drive a global climate change model MAGICC 6 [24] capable of reproducing global mean warming from complex GCMs. The resultant projections of global temperature change drive a pattern-scaling module ClimGen [25] capable of reproducing climate change patterns diagnosed from eighteen alternative GCM simulations combined with a baseline observed climate using the CRU TS 2.10 dataset. We produce 72 spatially explicit time-series projections of monthly mean, minimum and maximum temperatures, total monthly precipitation, wet day frequency and percentage of cloud cover downscaled to $0.5^\circ \times 0.5^\circ$ resolution ($\sim 50 \text{ km}^2$ at the Equator) and consistent with the RCPs [26]. Monthly mean climate data are interpolated to daily using a stochastic weather generator within PEGASUS (see appendix B).

Changes in temporal distribution of precipitation are scaled according to changes in global mean temperature using a gamma shape parameter such that ClimGen outputs of total monthly precipitation and wet day frequency account for changes in present and future precipitation variability [25]. Changes in monthly mean, minimum and maximum temperatures are estimated according to changes in global mean temperature so that the weather generator within PEGASUS generates warmer temperature extrema as global mean temperature increases. However, potential changes in the frequency of extreme temperature events are not yet simulated within ClimGen (see appendix B). As those might also change in future [27], results presented here might be more conservative than with fully realized changes in temperature variability (see section 7 for further discussion).

2.3. Global average yield and production estimates

Global average actual yield is calculated by combining yields simulated from full irrigation and no irrigation runs weighted by irrigated and rainfed areas. We consider three time periods averaged over 30 years: baseline corresponding to the 1980s (1971–2000), medium time horizon corresponding to the 2050s (2036–2065) and long time horizon corresponding to the 2080s (2071–2100). Total production is estimated by multiplying actual yield by corresponding harvested area assuming harvested area remains constant as present-day using the Earthstat dataset [20].

We use the World Bank definition to classify countries by income level: Economies are divided according to 2012 GNI per capita, calculated using the World Bank Atlas method [28]. The groups are: low income, \$1035 or less; lower middle income, \$1036–\$4085; upper middle income, \$4086–\$12 615; and high income, \$12 616 or more. We calculated country-level production for the year 2000 (average over the six-year period: 1997–2002) using the CRU TS 2.10 climate dataset and selected the top-five producing countries according to PEGASUS yield estimates multiplied by crop harvested area. The top-five countries for maize and soybean production agree with the United Nations Food and Agriculture Organization (FAO) rankings [29] for the year 2000. In the case of spring wheat, we use spring wheat harvested area generated by combining wheat harvested area [20] and global spring wheat planting and harvesting calendar [30], assuming that farmers do not grow both winter and spring varieties in the same location.

2.4. Representative concentration pathways and climate change futures

The four RCPs encompass a mitigation pathway in which radiative forcing is reduced to 2.6 W m^{-2} (RCP 2.6) by 2100, a *business as usual* pathway in which radiative forcing increases to 8.5 W m^{-2} (RCP 8.5) by 2100, and two stabilization pathways in which forcing levels out at 4.5 W m^{-2} (RCP 4.5) and 6.0 W m^{-2} (RCP 6.0) by 2100 respectively. The Fifth Assessment Report (AR5) of the IPCC reports RCP 2.6 engenders a world with global mean surface temperature stabilized at 1°C by the 2050s with respect to 1986–2005 [27], resulting in moderate heat stress and low CO_2 fertilization effects. Similarly, RCP 8.5 leads to a global mean warming exceeding 1.4°C and up to 4.8°C by the 2080s [27], along with unprecedented extreme heat stress and high potential CO_2 fertilization effects.

Here we evaluate and explore uncertainties in crop sensitivity to direct physiological effects of increased CO_2 and HSA for the two most contrasting RCPs (i.e., RCP 2.6 and 8.5). Consequently, results presented consist of 72 simulations to account for combined impacts of mean climate change, extreme temperatures around crop anthesis (HSA), and direct CO_2 fertilization effects (CO_2) denoted as CC, 36 simulations to account for impacts of mean climate change and direct CO_2 fertilization only ($\text{CC}_{w/o} \text{ HSA}$), and 36 simulations to account for impacts of mean climate change and extreme temperatures only ($\text{CC}_{w/o} \text{ CO}_2$), for each of the three crops.

3. Global average trends

We find global average yield decreases for all maize simulations (ΔY ranges from $-2.9 \pm 2.6\%$ under RCP 2.6 to $-12.8 \pm 6.7\%$ under RCP 8.5 by the 2080s for CC) whereas corresponding yields of spring wheat and soybean, when CO_2 fertilization effects are included, increase throughout the 21st century owing to large positive responses in C_3 crops (ΔY ranges from $9.9 \pm 3.6\%$ under RCP 2.6 to $34.3 \pm 13.5\%$ under RCP 8.5 for spring wheat and from $7.1 \pm 7.0\%$ under RCP 2.6 to $15.3 \pm 26.5\%$ under RCP 8.5 for soybean by the 2080s for CC) (figure 1 and table 1). HSA strongly influences maize and spring wheat yields, contributing to nearly half of expected losses for maize by the 2080s under RCP 8.5 ($\Delta Y = -12.8 \pm 6.7\%$ for CC compared to $\Delta Y = -7.0 \pm 5.3\%$ for $\text{CC}_{w/o} \text{ HSA}$) and substantial reductions in expected yield gains for spring wheat ($\Delta Y = 34.3 \pm 13.5\%$ for CC compared to $\Delta Y = 72.0 \pm 10.9\%$ for $\text{CC}_{w/o} \text{ HSA}$). In contrast, HSA moderately affects soybean global yield trajectories due to its higher critical temperature threshold to HSA (see Methods and appendix A) ($\Delta Y = 15.3 \pm 26.5\%$ for CC compared to $\Delta Y = 20.4 \pm 22.1\%$ for $\text{CC}_{w/o} \text{ HSA}$). Soybean exhibits a larger range of results spanning both positive and negative outcomes globally whereas maize results are mostly negative and wheat results mostly positive with CO_2 fertilization effects. Differences between crop responses and the larger range of results for soybean reflect differences in specific temperature tolerance to HSA (e.g. soybean has higher critical temperature tolerance but lower limit temperature

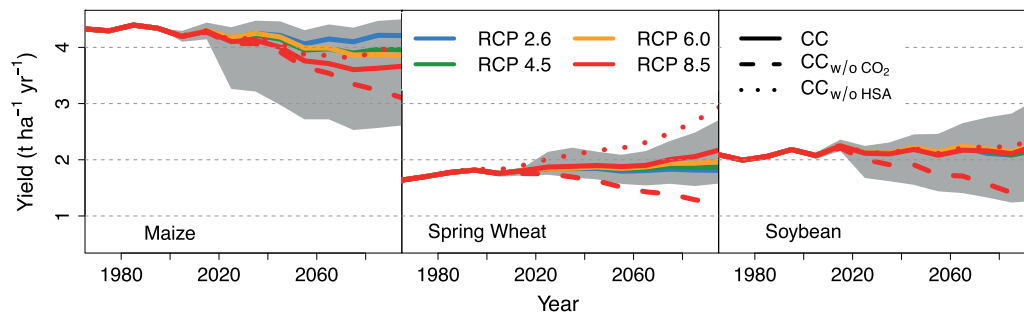


Figure 1. Global average yield trends simulated by PEGASUS under all 4 RCPs \times 18 GCMs ensemble for maize, spring wheat and soybean. Thick lines represent median value across each set of simulations. Full lines are for simulations including both CO₂ fertilization effect and HSA (CC). Dotted lines are for simulations not taking into account HSA (CC_{w/o} HSA) and dashed lines are for simulations with no CO₂ fertilization effects (CC_{w/o} CO₂). Grey areas represent the range of global average yield estimates in the case of CC simulations.

Table 1. Median of relative change in global crop yield ΔY (%) by the 2050s and the 2080s relative to the 1980s for maize, spring wheat, and soybean derived from 30-year average yield calculated for each period. The range represents the median absolute deviation (MAD) from median.

Crop sensitivity	RCP	Maize		Spring wheat		Soybean	
		2050	2080	2050	2080	2050	2080
CC	RCP 2.6	-3.1 ± 2.4	-2.9 ± 2.6	9.8 ± 3.0	9.9 ± 3.6	9.5 ± 7.3	7.1 ± 7.0
	RCP 4.5	-4.9 ± 3.3	-6.8 ± 4.2	13.0 ± 4.0	16.7 ± 5.3	10.8 ± 8.9	9.4 ± 12.6
	RCP 6.0	-4.2 ± 3.1	-8.3 ± 5.2	13.3 ± 3.7	23.0 ± 6.8	11.4 ± 8.4	13.0 ± 16.1
	RCP 8.5	-7.4 ± 3.2	-12.8 ± 6.7	16.9 ± 6.3	34.3 ± 13.5	11.1 ± 12.5	15.3 ± 26.5
CC _{w/o} HSA	RCP 2.6	-2.2 ± 2.1	-2.2 ± 2.1	16.6 ± 3.1	15.9 ± 3.4	10.2 ± 7.1	7.7 ± 6.8
	RCP 8.5	-4.7 ± 3.3	-7.0 ± 5.3	31.9 ± 4.9	72.0 ± 10.9	12.4 ± 11.6	20.4 ± 22.1
CC _{w/o} CO ₂	RCP 2.6	-4.7 ± 2.4	-4.4 ± 2.5	-4.5 ± 3.3	-2.9 ± 3.5	1.9 ± 6.8	0.9 ± 6.6
	RCP 8.5	-10.5 ± 3.2	-22.0 ± 5.7	-10.1 ± 5.0	-24.1 ± 7.1	-6.9 ± 9.6	-26.0 ± 17.3

tolerance in comparison to maize—see appendix A) as well as differences in GCM precipitation and temperature patterns and in spatial patterns of production specific to each crop. Figure S2 in the SI (available at stacks.iop.org/ERL/9/034011/mmedia) illustrates level of agreement in GCM simulations for each crop. In the case of soybean, there are as many areas showing a net decrease in yield as there are showing a net increase. However, in some important soybean production areas such as the USA and Brazil, there is no agreement on whether the sign of the projected yield changes is positive or negative (see also section Spatial patterns).

When CO₂ fertilization effects are excluded from simulations (dashed lines in figure 1), spring wheat and soybean yields follow maize's negative trend, soybean being the most affected crop: $\Delta Y = -26 \pm 17.3\%$ for soybean, $\Delta Y = -22.0 \pm 5.7\%$ for maize, and $\Delta Y = -24.1 \pm 7.1\%$ for spring wheat respectively for RCP 8.5 by the 2080s (see table 1). Soybean also shows the widest range of simulated yields when including HSA with and without CO₂ effects.

Maize is by far the most negatively affected crop and our results suggest a climate change future following RCP 2.6 could avoid fairly significant losses otherwise expected with higher RCPs, due to their larger heat and water stress conditions—since CO₂ fertilization effects are minimal for maize, a C₄ crop. On the contrary, spring wheat and soybean, both C₃ crops, could benefit greatly from higher CO₂ concentration in the atmosphere arising from RCP 8.5 or RCP 6.0 as,

in these cases, beneficial CO₂ fertilization effects outweigh negative effects of mean climate change and extremes. However, crop response to elevated CO₂ remains the largest source of uncertainty as little is known about their actual response in the field throughout the world, especially under tropical climatic conditions and varied soil nutrient availability (all experiments to date have been conducted either in chambers or in fields located in the United States and in Europe, i.e., under temperate climatic conditions—see Discussion).

Finally, maize, spring wheat and soybean have different tolerance thresholds to extreme temperatures (see appendix A), leading to substantial differences in yield response. Spring wheat is the most affected by extreme temperatures and soybean is the least affected. By the 2080s for RCP 8.5, HSA accounts for 45% of total negative impacts on maize, offsets 25% of positive impacts on soybean and 52% of positive impacts on spring wheat when averaged at the global scale (table 1).

4. Spatial patterns

We confirm previous findings of regional disparities in crop yield impacts, with yield increases in high latitudes and large yield reductions in mid and low latitudes (figure 2). Maize, with the largest cultivated area, shows a uniform decrease in yield over mid and low latitudes by the 2080s (figure 2(a)).

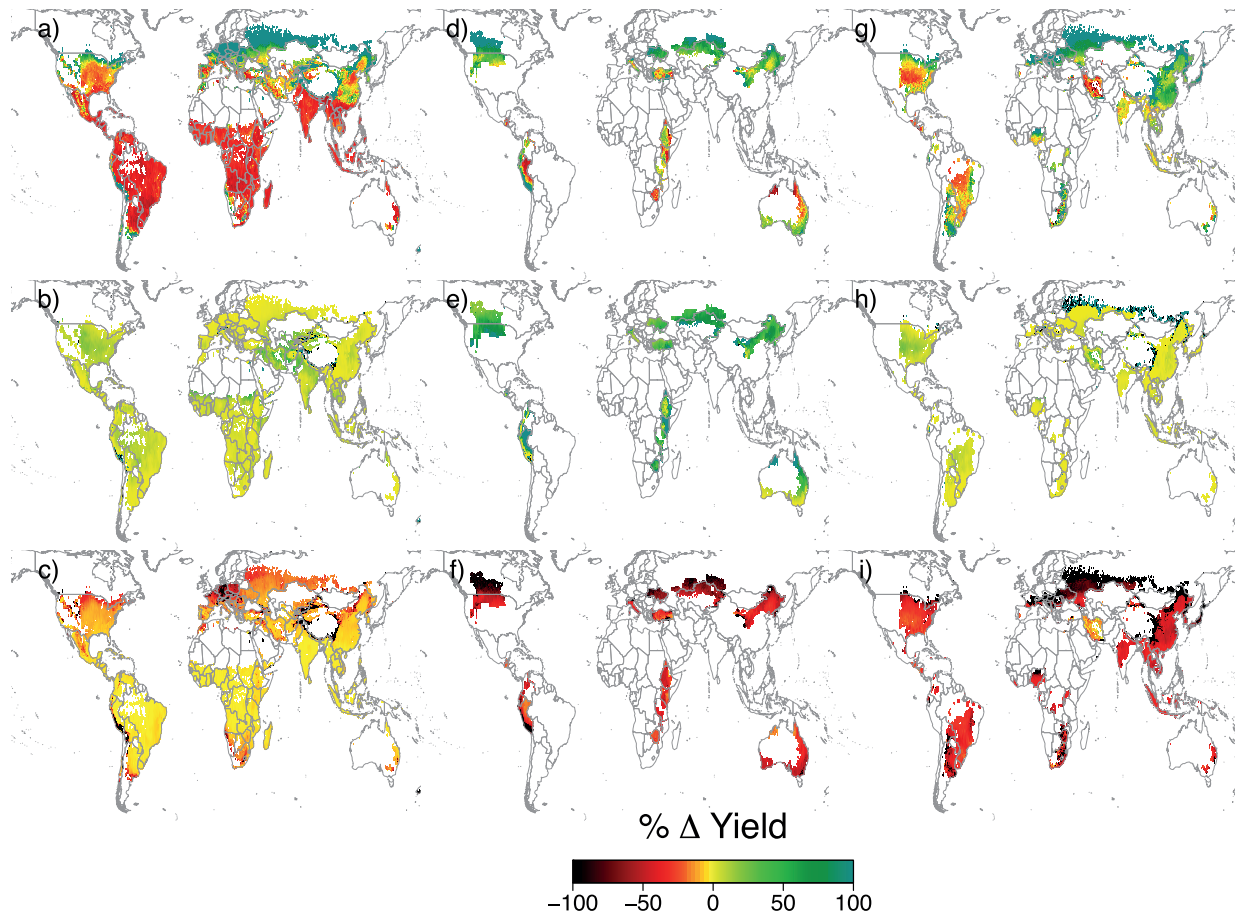


Figure 2. Maps of median ΔY (%) across the 18 GCMs ensemble for RCP 8.5 in the 2080s relative to the 1980s for maize (a), spring wheat (d) and soybean (g). Maps ((b)–(e)–(h)) show corresponding ΔY differences (%) between $CC_{w/o}$ HSA and CC simulations (green areas show important yield gains without HSA). Similarly, maps (c-f-i) show corresponding ΔY differences between $CC_{w/o}$ CO_2 and CC simulations (red to black areas show important yield losses without CO_2 fertilization).

In contrast, spring wheat and soybean present disparate results owing to contradictory effects resulting from beneficial CO_2 fertilization and detrimental extreme heat stress, the latter playing a critical role in some regions (figures 2(d) and (g) respectively). The number of simulations agreeing in the sign of change in yield is also higher for maize than for the other crops (see figure S1 in the SI (available at stacks.iop.org/ERL/9/034011/mmedia), which presents corresponding maps of ensemble simulations and their agreement).

Comparison between maps from top (CC) and middle ($CC_{w/o}$ HSA) rows in figure 2, indicates crop harvested areas at risk of HSA. In the case of maize (figures 2(a) and (b)), greater HSA sensitivity occurs in the American corn-belt, the Middle-East, west and south Asia, and northeast China. Within the top-five producing countries (figure 3), Brazil, Mexico and Argentina experience large decreases in national production, exacerbated by HSA (blue and yellow bars). The United States also faces a notable decrease in all simulations. China's small gain owing to CO_2 fertilization effects is cancelled out by HSA. These losses among the top-five producing countries (i.e., accounting for 80% of global maize production) could play a major role in future world supply of maize, with consequences

for stability of international crop markets and higher risks of future food insecurity as already experienced during the 2008 global food crisis [31, 32].

In the case of spring wheat (figures 2(d) and (e)), all current cultivated areas experience heat stress damage: the most severely impacted regions are again the mid and low latitudes, including the northern part of the United States, the Near-East and eastern part of Australia. In fact, all top-five producing countries exhibit drastic reductions in anticipated production increases due to HSA (figure 3). Note country ranking is estimated according to PEGASUS spring wheat harvested area [30], which does not include winter wheat and hence differs from country rankings that include both winter and spring wheat (see Methods).

Finally, in the case of soybean (figures 2(g) and (h)), the United States, Brazil and India (accounting for more than 60% of global soybean production) are the most affected among the top-five producing countries (figure 3). In contrast, Argentina, the third largest soybean producing country, shows a large increase in its production, which could increase its ranking to second in terms of world production, before Brazil. China also displays large gains in production but only

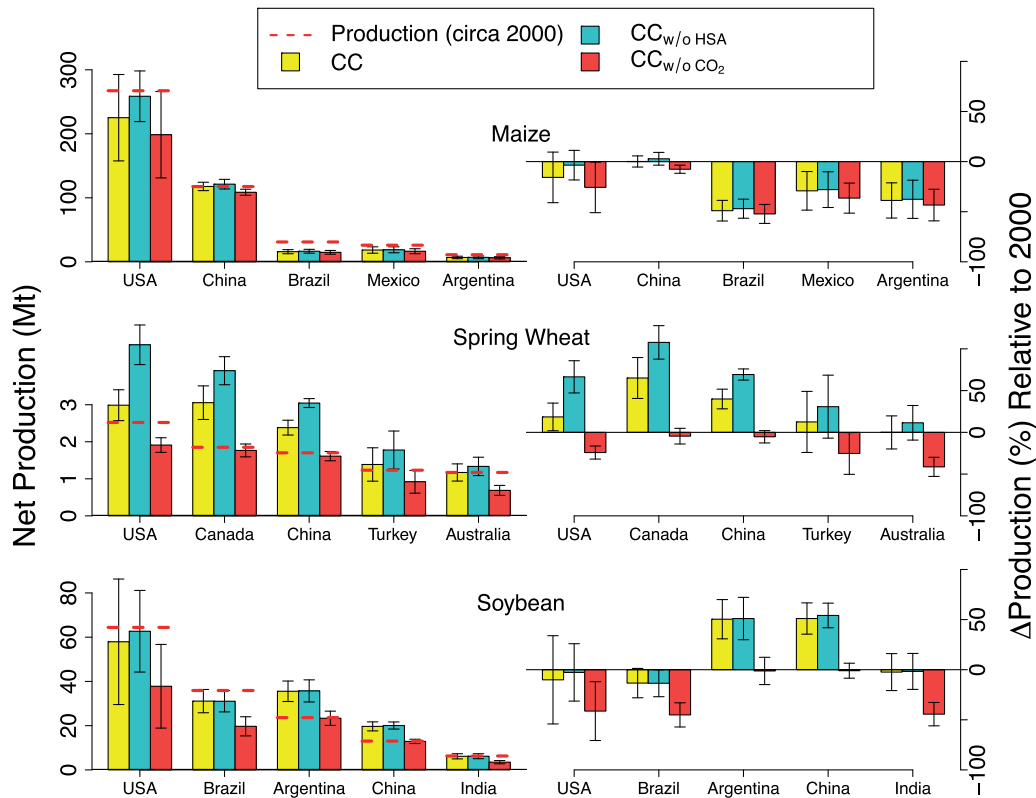


Figure 3. Bar plots showing net production (left side) and relative change in production (right side) for RCP 8.5 by the 2080s among top-five producing countries for maize, spring wheat and soybean. The top of the bar stands for median value and whiskers show range for each data. Dashed red lines on the left plots show current level of production, circa the year 2000. Production is estimated using present-day harvested area.

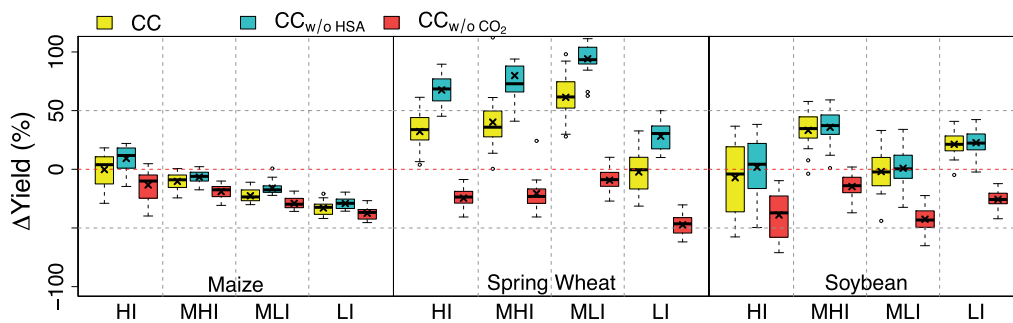


Figure 4. Box plots of ΔY (%) simulated for RCP 8.5 \times 18 GCMs for the 2080s relative to the 1980s among different income-level countries as defined by the World Bank: high income (HI), medium high income (MHI), medium low income (MLI) and low income (ML) levels for maize, spring wheat and soybean. The bottom and top of the box are lower and upper quartiles, respectively, the band near the middle of the box is the median value across each set of simulations, and the cross is the mean value.

when CO_2 fertilization effects are included and little change under $\text{CC}_{\text{w/o CO}_2}$. Finally, the main region of production, the central part of the United States, faces the most critical HSA effects.

When CO_2 fertilization effects are not taken into account (figures 2(c), (f) and (i)), yields of all three crops decrease uniformly in mid and low latitudes whereas changes in yields in high latitudes remain positive. In addition, we find a net decrease in yields for the top-five producing countries of each crop, including even Canada, a high latitude country, in the case of spring wheat (red bars in figure 3).

5. Country income levels

Impacts by the 2080s follow a regular gradient among income levels of nations (as defined by the World Bank [28]—see Methods) for maize and partly for spring wheat, whereas impacts are mixed in the case of soybean (figure 4). For maize, we find high income (HI) economies face the least damage while low income (LI) ones suffer the most. As seen in the global average trends (figure 1), maize yields decrease under nearly all simulations.

For spring wheat, yields increase from HI to medium low income (MLI) countries when CO_2 fertilization effects

are included. LI countries are less positively affected. Under $CC_{w/o} CO_2$, yields decrease the most for LI and HI groups. Spring wheat displays the strongest response to CO_2 fertilization effects and greater HSA compared to the other crops.

In the case of soybean, medium high income (MHI) countries experience large increases in yield when including CO_2 effects and small decreases under $CC_{w/o} CO_2$. LI economies also experience a small increase in yield when including CO_2 effects and a decrease without it. HI and MLI economies are the most impacted regions experiencing a large decrease in yield under $CC_{w/o} CO_2$, which is cancelled out with positive CO_2 fertilization effects. Spread in the results is similar within all groups, whereas HI economies exhibit larger uncertainties in impacts, which is also the case for maize.

Apart from maize, which shows greater impacts with decreasing income level, we find relative differences in results due to HSA or CO_2 fertilization effects do not show systematic patterns by income levels and repeat global trends illustrated in figures 1 and 2.

6. RCPs trajectories

PEGASUS is more responsive to CO_2 effects and HSA than different pathways of radiative forcing. Yet CO_2 effects on C_3 and C_4 crops vary greatly, resulting in quite different outcomes depending on crop–RCP combination. When all factors are taken into account, global average maize yield by the 2080s displays much greater reduction under RCP 8.5 ($\Delta Y = -12.8 \pm 6.7\%$) than under RCP 2.6 ($\Delta Y = -2.9 \pm 2.6\%$), and moderate losses under RCP 4.5 ($\Delta Y = -6.8 \pm 4.2\%$) and 6.0 ($\Delta Y = -8.3 \pm 5.2\%$) (figure 1). In contrast, yields of spring wheat and soybean increase the most under RCP 8.5 (up to $34.3 \pm 13.5\%$), followed by RCP 6.0 (up to $23.0 \pm 6.8\%$), RCP 4.5 (up to $16.7 \pm 5.3\%$) and RCP 2.6 (up to $9.9 \pm 3.6\%$). By the 2050s, maize yield may be a little higher under RCP 4.5 than under RCP 6.0. Similarly, soybean yield could be slightly higher under RCP 6.0 than RCP 8.5. These differences highlight the complexity of crop–climate– CO_2 interactions.

Relative changes in production (figure S3 in the SI available at stacks.iop.org/ERL/9/034011/mmedia for top-five countries) and yield (figure S4 in the SI available at stacks.iop.org/ERL/9/034011/mmedia for income-level groups) under RCP 2.6 are much smaller than under RCP 8.5 (figures 3 and 4 respectively). However, the range of uncertainties is greatly reduced. A strong mitigation scenario resulting in a low stabilized radiative forcing (i.e., RCP 2.6) could therefore contribute to reduced uncertainties in projections of overall impacts and thus facilitate adaptation planning. In contrast, a *business as usual* future such as RCP 8.5 is associated with large uncertainties in projected impacts, and designing adaptation strategies for such an uncertain future is much more challenging.

Finally, when assuming CO_2 fertilization to be negligible (i.e., $CC_{w/o} CO_2$), we find dramatic yield losses for all three crops by the 2080s under RCP 8.5; whereas corresponding yield losses are reduced by more than 80% under RCP 2.6 (see two last rows in table 1). In this case, our findings

present major differences between RCP trajectories and further emphasize the importance of better quantifying the role of elevated atmospheric CO_2 on crops (see discussion, section 7).

7. Discussion and conclusion

Our paper fills an important gap in previous assessments of climate change impact on global crop yield by simulating, for the first time at the global scale, effects of extreme heat stress during the crop reproduction phase and an extensive range of future climate scenarios (72) encompassing differences in GHG emissions and GCMs. Table 2 compares key results presented here against other global scale impact assessments. We identified studies using different crop simulation approaches, including the LPJmL model [4], the DSSAT suite of crop models [6, 7] and version 1.0 of PEGASUS [5] under climate change only (referred to in the table as $CC_{w/o} HSA, CO_2$) and $CC_{w/o} HSA$ scenarios. Table 2 also includes results from a statistical model using historical observed data [33]. PEGASUS 1.1 differs from 1.0 by including an improved interpolation algorithm of monthly climate data to daily values using a weather generator and being sensitive to specific extreme heat stress (see Method section and appendix A). Some studies reported results for each individual crop and some reported multi-crop averages. Effects of HSA in PEGASUS 1.1 lead to more pessimistic outcomes. Importantly, PEGASUS 1.1 produces a wider range of estimated ΔY than any previous study. For instance, impacts on soybean yields may be largely positive or negative even when CO_2 fertilization effects are taken into account. Previous studies listed in table 2 considered only two to four GCMs to drive their crop models, whereas our study, using PEGASUS 1.1, takes into account an ensemble of eighteen GCMs, which increases the range of uncertainties, due to climate model scenarios.

Our results include some important scientific uncertainties and assumptions. First, we use global values of temperature thresholds for HSA for each crop whereas in reality temperature thresholds vary not only among crop types but also among crop cultivars. Second, this analysis omits winter wheat and therefore gives only a partial assessment on total global wheat yield (spring wheat as simulated in PEGASUS accounts for 35% of total wheat harvested area). Third, PEGASUS does not include negative impacts related to crop pest and disease factors, which have yet to be explicitly examined in crop models [1], or crop interactions with pollutants such as ozone, and nutrient– CO_2 interactions. Fourth, our study assumes no adaptation in fertilizer application rates, which does not represent realistic scenarios of future fertilizer application rates. In fact, we constrain our analysis to focus on biophysical aspects of climate impacts without speculating on future developments in the world economy and trade and gain in yield due to improvements in agro-technologies. Adaptation scenarios taking into account future fertilizer application rates would require additional information on economy and trade, which is beyond the scope of this study. Similarly, irrigation scenarios here do not rely on actual water resources available, assuming water is available in irrigated cropland. A more realistic assessment would require linkage to a global water

Table 2. Comparison of changes in global crop yield relative to present-day $\Delta Y(\%)$ with previous assessments from peer reviewed literature. Wheat results for PEGASUS include only spring variety whereas the other studies include both winter and spring varieties. The range represents extrema of global average yield change reported in previous studies and estimated by PEGASUS 1.1. Median change in crop yield due to changes in temperature (T), precipitation (P) and CO₂ is reported for the statistical model.

Crop sensitivity	Model and reference	Number of scenarios	Time horizon	Maize	Wheat	Soybean	Multi-crops
T, P, CO ₂	Statistical model [33]	Historical	1980–2008	–4	–3	1	
CC _w /o HSA, CO ₂	LPJmL [4]	3 SRES × 4 GCMs	2050				[–8; –4]
	DSSAT (rainfed only) [6]	1 SRES × 2 GCMs		[–12; –2]	[–10; –4]		
	PEGASUS 1.0 [5]	2 SRES × 2 GCMs		[–12; –6]	[–10; –4]	[–26; –12]	
	PEGASUS 1.1	2 RCPs × 18 GCMs		[–16; –1]	[–20; –14]	[–33; 8]	[–11; 0]
CC _w /o CO ₂	LPJmL [4]	3 SRES × 4 GCMs	2050				[12; 13]
	PEGASUS 1.1	2 RCPs × 18 GCMs		[–11; 2]	[10; 86]	[–19; 25]	[–5; 26]
	PEGASUS 1.1	4 RCPs × 18 GCMs		[–13; 1]	[3; 52]	[–21; 24]	[–5; 18]
CC	PEGASUS 1.1	2 RCPs × 18 GCMs	2080	[–32; 0]	[–39; 3]	[–55; 7]	[–21; 3]
CC _w /o HSA	DSSAT [7]	7 SRES × 2 GCMs	2080				[–5; 1]
	PEGASUS 1.1	2 RCPs × 18 GCMs		[–15; 2]	[10; 121]	[–25; 46]	[–7; 26]
	PEGASUS 1.1	4 RCPs × 18 GCMs		[–25; 1]	[4; 60]	[–32; 44]	[–9; 22]
	PEGASUS 1.1	4 RCPs × 18 GCMs					

model, which could lead to reductions in irrigated crop yield due to water scarcity. Fifth, CO₂ fertilization effects on crops, which are included here, remain controversial [34–36]. Atmospheric CO₂ concentrations continue to rise rapidly, having recently surpassed 400 parts per million. The potential for CO₂ fertilization effects to alleviate the largely negative impacts of climate change on crops, and ultimately food security, is unclear. Little is known about actual crop response to elevated CO₂ effects in many parts of the world. Current Free-Air CO₂ Enrichment (FACE) experiments [37] have been conducted in temperate climates, principally in the United States and a few in Europe. CO₂ effects in tropical climates could be very different and possibly more sensitive to soil nutrient availability. Differences in the impacts found here with and without CO₂ fertilization highlight the urgency for further study of CO₂ effects on crops across agroecosystems [38]. In addition, elevated CO₂ is expected to reduce C–N ratios in crops, hence reducing the quality of grains by reducing the overall protein content [39]. Although this last point is paramount for global food security, CO₂ effects on grain protein content are omitted from current global crop models. Sixth, monthly temperature series generated within CIAS do not take into account changes in the frequency of extreme temperatures, which would increase risk of HSA. As a result, our simulation results are probably conservative and may underestimate the yield impact of extreme temperatures. Finally, our study uses only one crop model and therefore omits a key source of uncertainty in crop response to changing climate inputs. The need for research into uncertainties associated with different impact models is increasingly recognized [19, 40].

To conclude, our results quantify the importance of extreme weather events on crop yield and confirm regional disparities in climate change impacts. By the 2080s under RCP 8.5, we find strong HSA effects for maize (responsible for up to 45% of global average yield losses under RCP 8.5 by the 2080s relative to the 1980s) and spring wheat (responsible for up to 52% reduction of global average yield gains) and smaller consequences for soybean (responsible for up to 25% reduction of global average yield gains). Future GHG emission pathways are shown here to play an important role in determining future crop production. These results highlight the importance of climate mitigation to avoid important yield impacts. Strong radiative forcing, leading to a large increase in global mean temperature and hence higher extreme temperatures, will impact crops negatively in some of the regions contributing most to global production and across different income countries. The potential effects on global food prices and crop yield reduction in currently food insecure areas represent significant consequences for global food security. The wide range of impacts across regions underscores the need for carefully targeted adaptation responses including breeding and technology programmes for greater crop heat tolerance.

Acknowledgments

We are particularly grateful to Sudipta Goswami for his technical assistance in generating the climate data and to Tim Osborn and Craig Wallace for providing the latest version

of the ClimGen software (<http://www.cru.uea.ac.uk/~timo/limngen/>) used in generating the climate change scenario data. Funding was provided by the European Commission Collaborative Project FP7-ENV-2010.4.2.1-1, ERMITAGE, for the provision of the climate data from CIAS, a Tyndall Centre for Climate Change Research doctorate stipend to DD, a Natural Sciences and Engineering Research Council (NSERC) of Canada Discovery Grant to NR, and a Natural Environment Research Council of the United Kingdom fellowship to RW, along with financial support through the ERMITAGE project to JP and RW.

Appendix A. Crop modelling

PEGASUS is a light-use efficiency (LUE) type global crop model that integrates, in addition to climate, the effect of planting date decision and cultivar choice, irrigation, and fertilizer application on crop yield for maize, spring wheat and soybean [5]. PEGASUS 1.1 used in this study includes several improvements since version 1.0 to reflect multiple climate change impacts on crop yields. These include the effects of elevated atmospheric CO₂ concentration on photosynthesis rate and transpiration demand, specific heat stress at anthesis and a stochastic weather generator to create daily data from monthly climate inputs.

A.1. CO₂ effect on LUE coefficient

PEGASUS operates at a daily time-step. The LUE model assumes photosynthesis in unstressed conditions is proportional to incoming solar radiation. Additionally, temperature, soil moisture availability, and nutrient availability can limit daily net biomass production (P). P is expressed in mol C m⁻² s⁻¹ as:

$$P = \varepsilon \text{APAR} f_T f_W f_N \quad (\text{A.1})$$

where ε (mol C mol quanta⁻¹) is the LUE coefficient, APAR (mol quanta m⁻² s⁻¹) represents the daily average absorbed photosynthetically active radiation. f_T , f_W , and f_N are three limiting factors varying between 0 (high stress) and 1 (no stress) of daily mean temperature, daily soil moisture, and soil nutrient status, respectively. ε increases with CO₂ so that:

$$\varepsilon = \frac{100\text{CO}_2}{\text{CO}_2 + e^{r_1 - r_2 \cdot \text{CO}_2}} \quad (\text{A.2})$$

where CO₂ is the concentration of carbon dioxide in the atmosphere (ppm), and r_1 and r_2 are shape coefficients. The shape coefficients are calculated by solving equation (A.2) using two known points (ε_{amb} , CO_{2amb}) and (ε_{hi} , CO_{2hi}). ε_{amb} is tuned to simulate present-day global crop yield data at CO_{2amb} = 380 ppm as in Deryng *et al.*, (2011) [5]. At CO_{2hi} = 550 ppm, parameters are $\varepsilon_{hi} = 1.06 \times \varepsilon_{\text{amb}}$ for maize, $\varepsilon_{hi} = 1.13 \times \varepsilon_{\text{amb}}$ for wheat, and $\varepsilon_{hi} = 1.19 \times \varepsilon_{\text{amb}}$ for soybean according to free-air CO₂ enrichment (FACE) results [36]:

$$r_1 = \ln \left[\frac{\text{CO}_{2\text{amb}}}{0.01 \cdot \varepsilon_{\text{amb}}} - \text{CO}_{2\text{amb}} \right] + r_2 \cdot \text{CO}_{2\text{amb}} \quad (\text{A.3})$$

$$r_2 = \frac{\ln \left[\frac{\text{CO}_{2\text{amb}}}{0.01 \cdot \varepsilon_{\text{amb}}} - \text{CO}_{2\text{amb}} \right] - \ln \left[\frac{\text{CO}_{2hi}}{0.01 \cdot \varepsilon_{hi}} - \text{CO}_{2hi} \right]}{\text{CO}_{2hi} - \text{CO}_{2\text{amb}}} \quad (\text{A.4})$$

Table A.1. Temperature critic (T_{cr}) and limit (T_{lim}) (in °C) for maize, wheat and soybean used in this study (PEGASUS 1.1) and corresponding values found in the literature.

Reference	Maize		Wheat		Soybean	
	T_{cr} (°C)	T_{lim} (°C)	T_{cr} (°C)	T_{lim} (°C)	T_{cr} (°C)	T_{lim} (°C)
PEGASUS 1.1	32	45	25	35	35	40
Lobell <i>et al</i> (2013) [8]	30					
Moriondo <i>et al</i> (2011) [10]	31	40				
Semenov and Shewry (2011) [11]			27			
Teixeira <i>et al</i> (2011) [14]	35	45	27	40	35	40
Thuzar <i>et al</i> (2010) [45]					34	
Modhej <i>et al</i> (2008) [46]			22			
Spiertz <i>et al</i> (2006) [47]			25			
Porter and Gawith (1999) [48]			24	31		
Ferris <i>et al</i> (1998) [49]			25	35		

A.2. CO₂ effect on transpiration

The water stress factor f_w [5] depends on daily potential evapotranspiration demand (PET), which is reduced by CO₂ concentration following a similar and simplified approach to Easterling *et al* [41], also used in the SWAT and EPIC models [42, 43], so that:

$$PET = PET_{amb} \times \left(1.5 - 0.5 \frac{CO_2}{CO_{2amb}} \right) \quad (A.5)$$

where PET_{amb} corresponds to PET estimated under CO_{2amb} . While CO₂ effect on LUE coefficient is crop specific, CO₂ influence on PET is identical for all crops.

A.3. Heat stress at anthesis

Crops are sensitive to extreme temperatures, particularly around the reproductive stage, called anthesis. Following the methodology developed by Challinor *et al* [16] and used in several other studies [10, 14], PEGASUS' account of extreme temperature stress on crop yield follows three steps:

- estimation of the crop thermal sensitivity period (TSP);
- identification of an extreme temperature event according to crop specific temperature tolerance threshold;
- application of a heat stress factor f_{HSA} on storage organ production, which depends on duration and intensity of the high temperature event.

Crop TSP includes a couple of days before and after anthesis and is estimated as a function of crop growing period length (GPL), which depends on growing degree days accumulation [5] and varies with crop cultivars. Anthesis is scheduled when the number of days since emergence reaches half of crop GPL (calculated between emergence and maturity), i.e., 0.5 GPL; TSP starts a few days before anthesis at 0.45 GPL and ends after anthesis at 0.7 GPL. A high temperature event occurs when daily effective temperature (T_{eff}) exceeds a critical temperature (T_{cr}) threshold. Above this threshold, the daily heat stress factor f_{HSA} during the

TSP is calculated according to:

$$f_{HSA} = \begin{cases} 1 & \text{if } T_{eff} < T_{cr} \\ 1 - \frac{T_{eff} - T_{cr}}{T_{lim} - T_{cr}} & \text{if } T_{cr} \leq T_{eff} < T_{lim} \\ 0 & \text{if } T_{eff} \geq T_{lim} \end{cases} \quad (A.6)$$

T_{eff} is defined as $(T_{mean} + T_{max})/2$, where T_{mean} is the daily mean temperature and T_{max} is the daily maximum temperature [44], T_{lim} is the limit temperature above which f_{HSA} is maximal. Crop specific T_{cr} and T_{lim} come from a synthesis of values found in the literature [10, 11, 14, 33, 45–49] (table A.1). Temperature tolerance differs for each crop. Here, HSA critical temperature thresholds are 25 °C for spring wheat, 32 °C for maize and 35 °C for soybean. Hence, as temperatures increase spring wheat yield is impacted first, followed by maize and finally soybean. However, HSA impact functions differ among crop type as temperature thresholds at zero pod-set are 35 °C for spring wheat, 45 °C for maize and 40 °C for soybean.

The daily heat stress factor is accumulated and averaged over the TSP so that f_{HSA} is expressed as:

$$f_{HSA} = \frac{1}{TSP} \sum_i f_{HSAi} \quad (A.7)$$

Finally, crop yield (Y in t Ha⁻¹) affected by HSA is expressed as:

$$Y = \frac{EF}{0.45 DF} C_{so} \times f_{HSA} \quad (A.8)$$

where C_{so} represents the amount of dry carbon accumulated in the storage organs at harvesting date, EF is the economic fraction of the storage organs, DF is the dry fraction of the economic yield to convert weight of dry matter to weight of fresh matter, and 0.45 is the mass of carbon contained in one unit of dry matter [5].

Appendix B. Climate data and weather generator

B.1. CIAS

Monthly climate data used in this study comprise historical climate data from the CRU TS 2.10 dataset [17] and 72

global climate change patterns derived from eighteen GCMs combined with four RCPs generated using CIAS [23]: a modular integrated assessment model (IAM) linking an emission scenarios module (ESM), a simple global climate module (SCM), MAGICC 6 [24], and a climate scenario downscaling module (DSM), ClimGEN [25]. Designed for modelling climate change policy and effectiveness, CIAS is a unique multiinstitutional modular and flexible integrated assessment system offering a single framework to create multiple IAMs by interchanging the coupling of the different modules [23]. CIAS is supported by a software framework called SoftIAM, which allows various combinations of modules to be connected together into alternative IAMs and provides a graphical interface to let users interact with the system, configure and perform various kind of simulations to answer different scientific and policy questions. CIAS modules are configured to emulate here the behaviour of eighteen GCMs used in the IPCC AR4 [3] coupled to four RCPs used in the IPCC AR5 [18].

B.2. RCPs

The ESM provides atmospheric concentration data of GHG emissions for various scenarios database such as the IPCC SRES and RCPs, the latter being used in this study. Alternatively, GHG concentrations can be estimated from emission scenarios generated from an economic module linked to an emission converter as presented in [23]. GHGs concentration data are then input to MAGICC 6.

B.3. MAGICC

The MAGICC model [50] has been developed and updated over two decades and widely used in integrated modelling studies [51, 52]. MAGICC is a single piece of software comprising a set of linked internal components to simulate GHGs cycles, radiative forcing, and ice melt. Radiative forcing drives an upwelling diffusion energy balance model to estimate future climate changes. MAGICC 6 [24] is an updated version of the original MAGICC, with an improved representation of the carbon cycle. Climate feedback on the carbon cycle is included; the resulting $[CO_2]$ depends on the forcing, the climate sensitivity and the ocean heat uptake efficiency. Sulphate aerosol forcing is scaled directly with the emissions because of the short residence time in the atmosphere. Thus the model allows the user to emulate GCM output, specifically changes in $[CO_2]$, global-mean surface air temperature and sea level between the years 2000 and 2100 resulting from anthropogenic emissions of CO_2 , CH_4 , N_2O , HFCs, CFCs and PFCs, as well as SO_2 . MAGICC 6 is tuned to emulate here eighteen state-of-the-art GCMs to create global temperature projections for the four RCPs [18].

B.4. ClimGEN

The DSM generates spatially explicit climate data at various temporal scale from the single global-mean surface air temperature calculated by the SCM. The current DSM is CLIMGEN, which produces monthly, seasonal and annual mean climate data at a spatial resolution of $0.5^\circ \times 0.5^\circ$ grid-cell covering

both the terrestrial land surface excluding Antarctica [17]. CLIMGEN follows a pattern-scaling methodology currently based on the CMIP3 GCM patterns [26]: any given change in annual mean temperature as simulated by MAGICC 6 can be linearly rescaled to represent spatial and temporal pattern of change in each climate variables. ClimGEN combines these change patterns with the observed climatology, currently provided by the CRU TS 2.10 dataset [17], to produce patterns of mean absolute climate, and then combines them with observed time series of deviations from climatology to produce realisations of climate change over 2001 to 2100 with realistic yearly variability superimposed. CLIMGEN can generate monthly climate data for eight variables including mean, maximum and minimum temperatures, precipitation, vapour pressure, cloud cover and wet-day frequency. In the case of precipitation, change in GCM precipitation pattern is expressed as fractional change from present-day precipitation combined with the observed climatology by multiplication. To simulate future change in both precipitation variability and mean precipitation, ClimGEN includes a gamma shape parameter that represents the temporal distribution of precipitation. Change in the gamma shape parameter output by the GCMs is scaled by the required global-mean temperature change [25]. Future changes in the frequency of temperature extremes are not, however, as yet incorporated [25, 53].

B.5. Weather generator

Monthly climate data generated within CIAS are interpolated to a daily time-step using PEGASUS' internal weather generator. First, PEGASUS derives fraction of sunshine hours from CIAS cloud cover data following Doorenbos and Pruitt [54]. Then, PEGASUS uses monthly mean climate input of total precipitation, wet day frequency, fraction of sunshine hours and minimum, maximum and mean temperatures to feed into an extended version of the Richardson weather generator [55, 56]. Daily precipitation follows a two-states first order Markov chain according to the number of wet days per month and a gamma shape distribution of precipitation centred on monthly average precipitation per wet day [55, 57]. The method for wet and dry day transition probabilities is described in [58]. Daily temperature and fraction of sunshine hours follow a multivariate model for which mean and standard-deviation of each variable are tied to the wet or dry status of the day [57]. Furthermore, daily mean temperature estimates are tied to daily minimum and maximum temperature estimates [55], so that changes in daily mean temperatures reflect changes in minimum and maximum temperature extrema.

References

- [1] Gornall J et al 2010 Implications of climate change for agricultural productivity in the early twenty-first century *Phil. Trans. R. Soc. B* **365** 2973–89
- [2] Hillel D and Rosenzweig C 2010 Climate change and agroecosystems: main findings and future research directions *ICP Series on Climate Change Impacts, Adaptation, and Mitigation* vol 1 (*Handbook Of Climate Change And Agroecosystems Impacts, Adaptation, and Mitigation*) ed D Hillel and C Rosenzweig (London: Imperial College Press)

- [3] Easterling W E *et al* 2007 Food, fibre and forest products *Climate Change 2007: Impacts, Adaptation and Vulnerability. Contribution of Working Group II to the Fourth Assessment Report of the Intergovernmental Panel on Climate Change, ML*
- [4] Müller C, Bondeau A, Popp A, Waha K and Fader M 2010 WRD 2010: development and climate change *World Development Report* pp 1–12
- [5] Deryng D, Sacks W J, Barford C C and Ramankutty N 2011 Simulating the effects of climate and agricultural management practices on global crop yield *Glob Biochem. Cycles* **25** GB2006
- [6] Nelson G C *et al* 2010 *Food Security, Farming, and Climate Change to 2050* International Food Policy Research Institute (IFPRI)
- [7] Parry M, Rosenzweig C, Iglesias A, Livermore M and Fischer G 2004 Effects of climate change on global food production under SRES emissions and socio-economic scenarios. *Glob. Environ. Change* **14** 53–67
- [8] Lobell D B *et al* 2013 The critical role of extreme heat for maize production in the United States *Nature Clim. Change* **3** 1–5
- [9] Hawkins E *et al* 2013 Increasing influence of heat stress on French maize yields from the 1960s to the 2030s. *Global Change Biol.* **19** 937–47
- [10] Moriondo M, Giannakopoulos C and Bindi M 2011 Climate change impact assessment: the role of climate extremes in crop yield simulation *Clim. Change* **104** 679–701
- [11] Semenov M A and Shewry P 2011 Modelling predicts that heat stress and not drought will limit wheat yield in Europe *Sci. Rep.* **1** 66
- [12] Wahid A, Gelani S, Ashraf M and Foolad M R 2007 Heat tolerance in plants: an overview *Environ. Exp. Bot.* **61** 199–223
- [13] Gourdji S M *et al* 2013 Global crop exposure to critical high temperatures in the reproductive period: historical trends and future projections *Environ. Res. Lett.* **8** 024041
- [14] Teixeira E I, Fischer G, van Velthuisen H, Walter C and Ewert F 2011 Global hot-spots of heat stress on agricultural crops due to climate change *Agricult. Forest Meteorol.* **170** 206–15
- [15] Kirkham M B 2013 Research needs for agriculture under elevated carbon dioxide *ICP Series on Climate Change Impacts, Adaptation, and Mitigation* vol 2 (*Handbook of Climate Change And Agroecosystems Global and Regional Aspects and Implications*) ed D Hillel and C Rosenzweig (London: Imperial College Press)
- [16] Challinor A J, Wheeler T R, Craufurd P and Slingo J M 2005 Simulation of the impact of high temperature stress on annual crop yields *Agricult. Forest Meteorol.* **135** 180–9
- [17] Mitchell T D and Jones P D 2005 An improved method of constructing a database of monthly climate observations and associated high-resolution grids *Int. J. Climatol.* **25** 693–712
- [18] van Vuuren D P *et al* 2011 The representative concentration pathways: an overview *Clim. Change* **109** 5–31
- [19] Rosenzweig C *et al* 2013 Assessing agricultural risks of climate change in the 21st century in a global gridded crop model intercomparison *Global Climate Impacts: A Cross-Sector, Multi-Model Assessment Special Feature Proc. Natl Acad. Sci.* (doi: [10.1073/pnas.1222463110](https://doi.org/10.1073/pnas.1222463110))
- [20] Monfreda C, Ramankutty N and Foley J A 2008 Farming the planet: 2. Geographic distribution of crop areas, yields, physiological types, and net primary production in the year 2000 *Glob. Biogeochem. Cycles* **22** GB1022
- [21] Portmann F T, Siebert S and Döll P 2010 MIRCA2000 Global monthly irrigated and rainfed crop areas around the year 2000: a new high-resolution data set for agricultural and hydrological modeling *Glob. Biogeochem. Cycles* **24** GB1011
- [22] International Fertilizer Industry Association (IFA) 2002. Fertilizer Use by Crop, 5th edn (Rome: Food and Agric. Org., United Nations)
- [23] Warren R *et al* 2008 Development and illustrative outputs of the Community Integrated Assessment System (CIAS), a multi-institutional modular integrated assessment approach for modelling climate change *Environmen. Model. Softw.* **23** 592–610
- [24] Meinshausen M, Raper S C B and Wigley T M L 2011 Emulating coupled atmosphere-ocean and carbon cycle models with a simpler model, MAGICC6 Part 1: model description and calibration *Atmos. Chem. Phys.* **11** 1417–56
- [25] Osborn T J A 2009 *User guide for ClimGen: A flexible Tool for Generating Monthly Climate data sets and scenarios* vol 19 (Climatic Research Unit, University of East Anglia)
- [26] Meehl G A *et al* 2007 The WCRP CMIP3 multi-model dataset: a new era in climate change research *Bull. Am. Meteorol. Soc.* **88** 1383–94
- [27] Alexander L *et al* 2013 *Working Group I Contribution to the IPCC Fifth Assessment Report. Climate Change 2013: The Physical Science Basis. Summary for Policymakers, ML*
- [28] World Bank Country and Lending Groups <http://data.worldbank.org/about/country-classifications/country-and-lending-groups> (accessed on 21 July 2013)
- [29] Food and Agriculture Organization (FAO). FAOSTAT, Statistical Databases, <http://faostat.fao.org/default.aspx> (United Nations, Rome) (accessed 2013)
- [30] Sacks W J, Deryng D, Foley J A and Ramankutty N 2010 Crop planting dates: an analysis of global patterns *Global Ecol. Biogeogr.* **19** 607–20
- [31] Abbott P C, Hurt C and Tyner W E 2008 What's driving food prices? Farm Foundation
- [32] Piesse J and Thirtle C 2009 Three bubbles and a panic: an explanatory review of recent food commodity price events *Food Policy* **34** 119–29
- [33] Lobell D B *et al* 2011 Climate trends and global crop production since 1980 *Science* **333** 616–20
- [34] Ainsworth E A and Rogers A 2007 The response of photosynthesis and stomatal conductance to rising [CO₂]: mechanisms and environmental interactions plant *Cell Environ.* **30** 258–70
- [35] Tubiello F N *et al* 2007 Crop response to elevated CO₂ and world food supply: A comment on 'Food for Thought. . .' by Long *et al*, *Agricult. Water Manag.* **26** 215–23
- [36] Long S P 2006 Food for thought: lower-than-expected crop yield stimulation with rising CO₂ concentrations *Science* **312** 1918–21
- [37] Kimball B A 2010 Lessons from FACE: CO₂ effects and interactions with water, nitrogen and temperature *ICP Series on Climate Change Impacts, Adaptation, and Mitigation* vol 1 (*Handbook Of Climate Change And Agroecosystems Impacts, Adaptation, and Mitigation*) ed D Hillel and C Rosenzweig (London: Imperial College Press)
- [38] Leakey A D B, Bishop K A and Ainsworth E A 2012 A multi-biome gap in understanding of crop and ecosystem

- responses to elevated CO₂ *Curr. Opin. Plant Biol.* **15** 228–36
- [39] Taub D *et al* 2008 Effects of elevated CO₂ on the protein concentration of food crops: a meta-analysis *Global Change Biol.* **14** 565–75
- [40] Bassu S *et al* 2014 How do various maize crop models vary in their responses to climate change factors? *Global Change Biol.* at press doi: [10.1111/gcb.12520](https://doi.org/10.1111/gcb.12520)
- [41] Easterling D R *et al* 1992 Preparing the erosion productivity impact calculator (EPIC) model to simulate crop response to climate change and the direct effects of CO₂ *Agricult. Forest Meteorol.* **59** 17–34
- [42] Neitsch S L, Arnold J G, Kiniry J R and Williams J R 2005 Soil and water assessment tool. *Theoretical Documentation*, version 2005. Grassland, Soil and Water Research laboratory, Agricultural research service 808 East Blackland road, Temple, 808 East Blackland road, Temple, Texas 76502
- [43] Williams J R 1995 In *Computer Models of Watershed Hydrology* (Highlands Ranch, CO: Water Resources Publications) pp 909–1000 chapter 25 (The EPIC Model)
- [44] Penning de Vries F W T, Jansen D M, ten Berge H F M and Bakema A 1989 *Simulation of Ecophysiological Processes of Growth in Several Annual Crops* (Wageningen, Netherlands: Pudoc)
- [45] Thuzar M, Puteh A B, Abdullah N A P, Lassim M B M and Jusoff K 2010 The effects of temperature stress on the quality and yield of soya bean *J. Agricult. Sci.* **2** 1–8
- [46] Modhej A, Naderi A, Emam Y, Aynehband A and Normohamadi G 2008 Effects of post-anthesis heat stress and nitrogen levels on grain yield in wheat (T. durum and T. aestivum) genotypes *Int. J. Plant Production* **2** 257–67
- [47] Spiertz J H J *et al* 2006 Heat stress in wheat (Triticum aestivum L.): effects on grain growth and quality traits *Eur. J. Agron.* **25** 89–95
- [48] Porter J R and Gawith M 1999 Temperatures and the growth and development of wheat: a review *Eur. J. Agronomy* **10** 23–36
- [49] Ferris R, Ellis R, Wheeler T R and Hadley P 1998 Effect of high temperature stress at anthesis on grain yield and biomass of field-grown crops of wheat *Ann. Bot.* **82** 631
- [50] Wigley T M L and Raper S C B 2001 Interpretation of high projections for global-mean warming *Science* **293** 451–4
- [51] Rotmans J, Hulme M and Downing T E 1994 Climate change implications for Europe: An application of the ESCAPE model *Global Environ. Change* **4** 97–124
- [52] Van Vuuren D P *et al* 2008 Temperature increase of 21st century mitigation scenarios *Proc. Natl Acad. Sci. USA* **105** 15258–62
- [53] Warren R, Yu R M S, Osborn T J and de la Nava Santos S 2012 European drought regimes under mitigated and unmitigated climate change: application of the community integrated assessment system (CIAS) *Clim. Res.* **51** 105–23
- [54] Doorenbos J and Pruitt W O 1984 Guidelines for predicting crop water requirements *FAO Irrigation and Drainage Paper 24* (Rome: FAO)
- [55] Parlange M and Katz R W 2000 An extended version of the Richardson model for simulating daily weather variables *J. Appl. Meteorol.* **39** 610–22
- [56] Richardson C W and Wright D A 1984 WGEN: a model for generating daily weather variables, US Department of Agriculture, Agricultural Research Service, ARS–8
- [57] Richardson C W 1981 Stochastic simulation of daily precipitation, temperature, and solar radiation *Water Resour. Res.* **17** 182–90
- [58] Geng S 1986 A simple method for generating daily rainfall data *Agricult. Forest Meteorol.* **36** 363–76